THE JOURNAL OF BIOLOGICAL CHEMISTRY VOL. 287, NO. 33, pp. 27731–27742, August 10, 2012

Determinants of Interaction Specificity of the *Bacillus subtilis* GlcT Antitermination Protein

FUNCTIONALITY AND PHOSPHORYLATION SPECIFICITY DEPEND ON THE ARRANGEMENT OF THE REGULATORY DOMAINS[*] [S]

Received for publication, June 7, 2012, and in revised form, June 18, 2012 Published, JBC Papers in Press, June 21, 2012, DOI 10.1074/jbc.M112.388850

Sebastian Himmel[‡1], **Christopher P. Zschiedrich**[§1], **Stefan Becker**[‡1], **He-Hsuan Hsiao**[¶], **Sebastian Wolff**[‡], **Christine Diethmaier**[§], **Henning Urlaub**[¶‖], **Donghan Lee**[‡], **Christian Griesinger**[‡2], **and Jörg Stülke**[§3]

From the [‡]*Department of NMR-based Structural Biology and the* [¶]*Bioanalytical Mass Spectrometry Group, Max Planck Institute for Biophysical Chemistry, Am Fassberg 11, 37077 Göttingen, the* [§]*Department of General Microbiology, Georg-August-Universität Göttingen, Grisebachstrasse 8, D-37077 Göttingen, and* [‖]*Bioanalytics, Department of Clinical Chemistry, University Medical Center Göttingen, Robert Koch Strasse 40, 37075 Göttingen, Germany*

Background: The distinct proteins enzyme II and HPr phosphorylate the duplicated regulatory domains of the antitermination protein GlcT.
Results: HPr phosphorylates PRD2 much more readily than PRD1. Transposing the positions of PRD1 and PRD2 in GlcT can reverse this preference.
Conclusion: Steric/positional factors are largely responsible for phosphorylation specificity.
Significance: The conserved domain organization is crucial to achieve the desired control of GlcT activity.

The control of several catabolic operons in bacteria by transcription antitermination is mediated by RNA-binding proteins that consist of an RNA-binding domain and two reiterated phosphotransferase system regulation domains (PRDs). The *Bacillus subtilis* GlcT antitermination protein regulates the expression of the *ptsG* gene, encoding the glucose-specific enzyme II of the phosphotransferase system. In the absence of glucose, GlcT becomes inactivated by enzyme II-dependent phosphorylation at its PRD1, whereas the phosphotransferase HPr phosphorylates PRD2. However, here we demonstrate by NMR analysis and mass spectrometry that HPr also phosphorylates PRD1 *in vitro* but with low efficiency. Size exclusion chromatography revealed that non-phosphorylated PRD1 forms dimers that dissociate upon phosphorylation. The effect of HPr on PRD1 was also investigated *in vivo*. For this purpose, we used GlcT variants with altered domain arrangements or domain deletions. Our results demonstrate that HPr can target PRD1 when this domain is placed at the C terminus of the protein. In agreement with the *in vitro* data, HPr exerts a negative control on PRD1. This work provides the first insights into how specificity is achieved in a regulator that contains duplicated regulatory domains with distinct dimerization properties that are controlled by phosphorylation by different phosphate donors. Moreover, the results suggest that the domain arrangement of the PRD-containing antitermination proteins is under selective pressure to ensure the proper regulatory output, *i.e.* transcription antitermination of the target genes specifically in the presence of the corresponding sugar.

All organisms are exposed to ever-changing environments. To thrive successfully in a wide variety of conditions, all cellular activities have to be regulated. This regulation can take place at the level of gene expression or the level of the activity of the gene product. In bacteria, transcription is a major target of regulation. To achieve transcription regulation, the information of the environment must be sensed and has to be transduced to the transcription machinery. For this purpose, regulator proteins that either repress or activate transcription initiation or that control transcript elongation need to gather the relevant information. The modulation of the activity of regulator proteins may occur by direct interaction with low molecular weight effectors or other regulatory proteins, as well as by direct effects of the physicochemical conditions. These modes of control are exemplified by the *Escherichia coli* Lac repressor and the *Bacillus subtilis* CcpA and CtsR regulator proteins, respectively (1–3). Other regulators are controlled by post-translational modifications such as phosphorylation. This mechanism is most prominent in the bacterial two-component regulatory systems (4). Moreover, a class of regulators that control sugar metabolism is modulated by reversible phosphorylation mediated by proteins of the phosphoenolpyruvate:sugar phosphotransferase system (PTS).[4] All of these regulators contain two conserved PTS regulation domains (PRD1 and PRD2) that are the target of phosphorylation. These regulators may act as activators or antitermination proteins at the levels of transcription

* This work was supported by the Max Planck Society (to C. G.) and by Deutsche Forschungsgemeinschaft Grant SFB860 and the Fonds der Chemischen Industrie (to J. S. and C. G.).
[S] This article contains supplemental Figs. S1–S3.
[1] These authors contributed equally to this work.
[2] To whom correspondence may be addressed. Tel.: 49-551-201-2201; Fax: 49-551-201-2202; E-mail: cigr@nmr.mpibpc.mpg.de.
[3] To whom correspondence may be addressed. Tel.: 49-551-393781; Fax: 49-551-393808; E-mail: jstuelk@gwdg.de.

[4] The abbreviations used are: PTS, phosphotransferase system; PRD, PTS regulation domain; RBD, RNA-binding domain; Bis-Tris, 2-[bis(2-hydroxyethyl)-amino]-2-(hydroxymethyl)propane-1,3-diol; ESI, electrospray ionization; SP, sporulation.

TABLE 1
***B. subtilis* strains used in this study**
LFH, long flanking homology.

Strain	Genotype	Source[a]
168	*trpC2*	Laboratory collection
GP109	*trpC2 amyE*:: (*ptsG-lacZ aphA3*) Δ*glcT8*	Ref. 12
GP770	*trpC2 amyE*:: (*ptsG-lacZ cat*) Δ*glcT8*	QB7035 → GP109
GP771	*trpC2 amyE*:: (*ptsG-lacZ cat*)	pGP106 + GP770 → GP109
GP772	*trpC2 amyE*:: (*ptsG-lacZ cat*) *glcT H170D*	pGP128 + GP770 → GP109
GP773	*trpC2 amyE*:: (*ptsG-lacZ cat*) *glcT H172A*	pGP1583 + GP770 → GP109
GP776	*trpC2 amyE*:: (*ptsG-lacZ aphA3*) Δ*glcT-ptsG*::*tet*	GP926 → GP109
GP777	*trpC2 amyE*:: (*ptsG-lacZ aphA3*) Δ*glcT-ptsGHI*::*spc*	LFH-PCR → GP109
GP779	*trpC2 amyE*:: (*ptsG-lacZ cat*) *glcT H111D*	pGP102 + GP770 → GP109
GP926	*trpC2* Δ*glcT-ptsG*::*tet*	LFH-PCR → 168

[a] Arrows indicate construction by transformation.

initiation or elongation, respectively (5–7). The two classes of PRD regulators are exemplified by the *B. subtilis* activator LevR and the *E. coli* antitermination protein BglG (8–10).

We are interested in the control of glucose transport in the Gram-positive soil bacterium *B. subtilis*. Glucose is the preferred carbon source for these bacteria, and it is taken up by the PTS. The expression of the glucose-specific permease (also called enzyme II) is induced in the presence of glucose, and this induction is mediated by the GlcT antitermination protein (11). If glucose is available, active GlcT will bind to the nascent *ptsG* mRNA and stabilize the RNA antiterminator structure that prevents transcription termination (12, 13). In the absence of glucose, GlcT is phosphorylated by the glucose-specific enzyme II and thereby inactivated (14). As a result, elongation of the *ptsG* mRNA is terminated at a transcription terminator that is located between the transcription start and ribosome-binding sites.

GlcT is a member of the family of PRD-containing transcription antitermination proteins. These proteins are composed of an N-terminal RNA-binding domain (RBD) (13, 15) and two reiterated PRDs (5, 7, 16). The isolated RBD is sufficient to recognize and bind its RNA target and to cause transcription antitermination (12, 15). The two PRDs have different functions: PRD1 mediates the substrate-specific control of the antitermination proteins, whereas PRD2 is involved in the more general control of the proteins' activity by glucose and other preferred carbon sources (5, 7). If the specific sugar substrate is present, the corresponding enzyme II is engaged in the transport and concomitant phosphorylation of the sugar. In the absence of the substrate, the phosphorylated enzyme II accumulates and acts as a phosphate donor for PRD1 of the cognate antitermination protein. This phosphorylation in PRD1 results in the inactivation of the antitermination protein and therefore in transcription termination of the target gene. Thus, enzyme II has a dual activity as a transporter and a sensory protein. Therefore, it belongs to the trigger enzymes that combine metabolic and regulatory activities (17). Although PRD1 of each of the four *B. subtilis* antitermination proteins of this family (GlcT, LicT, SacT, and SacY) is assumed to be phosphorylated specifically by its cognate enzyme II, PRD2 of these proteins can be phosphorylated by the general phosphotransferase HPr (histidine-containing phosphocarrier protein) of the PTS. HPr receives a phosphoryl group at its His-15 from enzyme I of the PTS and can transfer this phosphoryl group to enzyme II of different families as well as to PRD-containing regulators and enzymes such as the glycerol kinase (7). In addition to His-15, the HPr protein of *B. subtilis* and other Gram-positive bacteria contains a second phosphorylation site, Ser-46. This site is phosphorylated in response to the quality of the carbon source by the metabolite-activated HPr kinase (18–20). The phosphorylation of Ser-46 inhibits the phosphorylation of His-15, and thus, no phosphate donor for PRD2 of the antitermination proteins is available in the presence of preferred carbon sources. As a result, the phosphorylation state of PRD2 depends on the available carbon sources. The catabolite-sensitive antiterminators LicT and SacT depend on HPr-dependent phosphorylation of PRD2 for activity. Similarly, HPr seems to activate the BglG antitermination protein of *E. coli* (21–23). In contrast, the *B. subtilis* antiterminators GlcT and SacY are active in the presence of glucose or high concentrations of sucrose. Therefore, these regulators have to be independent from HPr-dependent control of their PRD2. Indeed, these two proteins are active even in the absence of the HPr protein, and HPr-dependent phosphorylation of PRD2 results only in a slight increase in antitermination activity (14, 24).

From a structural point of view, the *B. subtilis* LicT antitermination protein is the most studied PRD-containing protein. For this protein, it has been shown that the two PRDs adopt similar folds and that the active LicT protein forms dimers, whereas monomeric LicT is inactive (Refs. 6, 25, and 26; see Ref. 27 for a review).

A major issue for the PRD-controlled antiterminators is specificity to allow a straight and appropriate flow of information. On the one hand, specificity is required to achieve interaction between the specific RNA antiterminator RNA and its cognate antitermination protein (28–30). On the other hand, specific interactions between the PTS components and their cognate PRDs are necessary to ensure the correct regulatory output.

In this work, we addressed the question of how HPr can discriminate between the two PRDs to achieve specific control of PRD2 of GlcT. *In vitro* studies revealed that HPr phosphorylates PRD1 with low efficiency and that phosphorylation of PRD1 controls the dimerization state of the domain. Moreover, using a truncated GlcT protein, we demonstrate *in vivo* that HPr can obtain access to a PRD only if the PRD is located at the C-terminal end of the antitermination protein. Thus, the dual regulation involving the two PRDs poses a selective pressure to conserve the domain arrangement in the PRD-controlled antitermination proteins.

EXPERIMENTAL PROCEDURES

B. subtilis Strains and Growth Conditions—All *B. subtilis* strains used in this work are derived from the laboratory wild-type strain 168. They are listed in Table 1. *B. subtilis* was grown in LB medium or CSE minimal medium containing succinate and glutamate/ammonium as basic sources of carbon and nitrogen, respectively (31). The medium was supplemented with auxotrophic requirements (at 50 mg/liter) and glucose as indicated. SP plates were prepared by the addition of 17 g of Bacto agar/liter (Difco) to SP medium.

DNA Manipulation and Transformation—E. coli DH5α (32) was used for cloning experiments. Transformation of *E. coli* and plasmid DNA extraction were performed using standard procedures (32). Restriction enzymes, T4 DNA ligase, and DNA polymerases were used as recommended by the manufacturers. DNA fragments were purified from agarose gels using the QIAquick PCR purification kit (Qiagen). *Phusion* DNA polymerase was used for the polymerase chain reaction as recommended by the manufacturer. DNA sequences were determined using the dideoxy chain termination method (32). All plasmid inserts derived from PCR products were verified by DNA sequencing. Chromosomal DNA of *B. subtilis* was isolated as described (31).

Transformation and Phenotypic Analysis—B. subtilis was transformed with plasmid or chromosomal DNA according to the two-step protocol described previously (33). Transformants were selected on SP plates containing chloramphenicol (5 μg/ml), kanamycin (10 μg/ml), spectinomycin (100 μg/ml), or tetracycline (10 μg/ml).

Quantitative studies of *lacZ* expression in *B. subtilis* were performed as follows. Cells were grown in LB medium and harvested throughout growth. β-Galactosidase-specific activities were determined with cell extracts obtained by lysozyme treatment as described previously (33). One unit of β-galactosidase is defined as the amount of enzyme that produced 1 nmol of *o*-nitrophenol/min at 28 °C.

Construction of Plasmids That Allow Expression of GlcT Variants—GlcT variants with changed domain arrangements were expressed in *B. subtilis* under control of the constitutively active $degQ^{hy}$ promoter using the expression vector pBQ200 (34). Briefly, the desired *glcT* alleles were generated by fusion PCR using oligonucleotides. The PCR products were digested with BamHI and HindIII and cloned into pBQ200 linearized with the same enzymes. Point mutations were introduced using the combined chain reaction with phosphorylated mutagenesis primers as described previously (35).

Construction of Deletion and Complementation Strains—Deletion of the *glcT ptsG* and *glcT ptsGHI* chromosomal region genes was achieved by transformation with PCR products constructed using oligonucleotides to amplify DNA fragments flanking the region to be deleted (corresponding to the *ykvZ* and *ptsHI* genes or *ykvZ* and *splAB* genes, respectively) and the intervening tetracycline or spectinomycin resistance cassette (36) as described previously (37).

Purification of Recombinant Proteins—Overexpression and purification of enzyme I, HPr, and PRD1 (uniformly ^{15}N-labeled) were carried out as described previously (38). Unlabeled PRD1 was produced in LB medium. RBD-PRD1 and GlcT H218D/H279D were cloned into a modified pET28a expression vector (Novagen), and after proteolytic cleavage of the His tag by tobacco etch virus protease, the proteins were purified following the protocol described for enzyme I and HPr (38). Proteins for mass spectrometric analysis were purified in 200 mM ammonium acetate and 2 mM DTT (pH 7.4).

In Vitro Protein Phosphorylation—The protein phosphorylation mixture was prepared as follows if not indicated otherwise. The target proteins (considered as monomers) were mixed with HPr in an equimolar ratio; enzyme I and phosphoenolpyruvic acid trisodium salt (Sigma-Aldrich) were added in 0.033 ratio and 20 to 100-fold excess, respectively. The phosphorylation reaction was carried out for 60–120 min at 37 °C. Phosphorylation for mass spectrometric experiments was performed in 40 mM ammonium acetate and 2 mM DTT (pH 7.4), and phosphoenolpyruvic acid tricyclohexylammonium salt (Sigma-Aldrich) was used as the phosphoryl group donor.

NMR Spectroscopy—NMR experiments were carried out at 30 °C using a 700-MHz NMR magnet equipped with an AVANCE I console and a TXI probe. ^{1}H,^{15}N heteronuclear single quantum correlation spectra were recorded with 64 (^{15}N) and 512 (^{1}H) complex points with $t_{1\max}$ = 32.2 ms and $t_{2\max}$ = 52.5 ms accumulating either 28 or 56 scans. The carrier frequencies were set to 117 ppm (^{15}N) and 4.7 ppm (^{1}H). NMR spectra were processed with TOPSPIN 2.0 (Bruker). The PRD1 concentration was between 0.2 and 0.4 mM. Protein phosphorylation and NMR experiments were performed in 200 mM NaCl, 50 mM Tris-HCl, 10 mM $MgCl_2$, and 2 mM DTT (pH 7.4).

Mass Spectrometric Analysis—After phosphorylation, the reaction mixture (molar ratios: PRD1 (1)/enzyme I (0.025)/HPr (1)/enzyme II (0.033)) was separated by electrophoresis on a 4–12% NuPAGE® Novex Bis-Tris gel system (Invitrogen) and stained with Coomassie Blue. PRD1 of GlcT was excised from the gel, digested with modified trypsin (Promega) at 37 °C overnight, and subsequently dried down with a SpeedVac concentrator. The tryptic peptides were dissolved in 50% acetonitrile for further MS analysis. MS analysis was performed on an LTQ Orbitrap mass spectrometer (Thermo Fisher Scientific) equipped with a nanoelectrospray ion source. MS conditions were as follows: spray voltage, 1.2 kV; heated capillary temperature, 150 °C; and normalized collision-induced dissociation collision energy, 37.5% for LTQ mass spectrometer. An activation of q = 0.25 and activation time of 30 ms were used. MS and MS/MS spectra were acquired in the Orbitrap mass spectrometer with resolution r = 30,000 at m/z 400 after accumulation to target values of 1,000,000 and 100,000, respectively.

Electrospray ionization (ESI) MS was performed with the PRD1 phosphorylation mixture (H172A variant), which was directly sprayed into a Micromass ZQ 4000 instrument (Waters) equipped with a single quadrupole detector. The phosphorylation mixture was infused at a flow rate of 10 μl/min and measured with 54 scans/min at a potential of +30 V. Signals were recorded between m/z 500 and 3000.

Size Exclusion Chromatography—Size exclusion chromatography was performed to analyze the aggregation states of the proteins. Chromatography runs were carried out on a Superdex 75 16/60 column (GE Healthcare) at 4 °C for PRD1 and on a

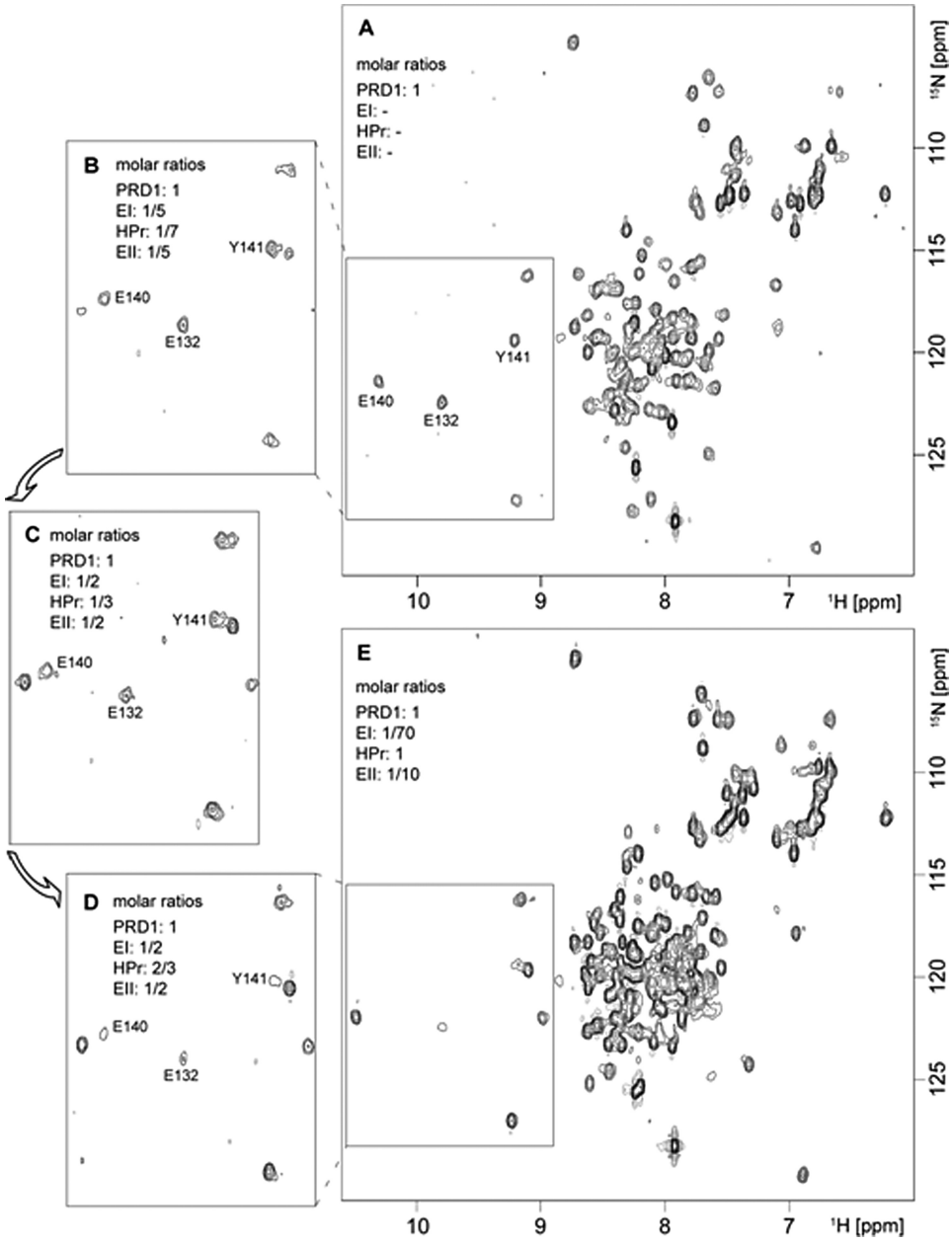

FIGURE 1. **HPr-dependent PRD1 phosphorylation monitored by NMR.** A series of ^{1}H,^{15}N heteronuclear single quantum correlation spectra shows the gradually increasing phosphorylation of isolated PRD1. *A*, the spectrum of non-phosphorylated PRD1. *B–D*, spectra of PRD1 phosphorylation mixtures, which contained different compositions of phosphorylation enzymes as indicated in the *insets*. The phosphorylation effect can be observed by additional and shifted amide resonances. A selection of resonances (Glu-140, Glu-132, and Tyr-141) highlights the spectral changes upon phosphorylation. *E*, the spectrum of nearly completely phosphorylated PRD1. Phosphorylation of PRD1 was maximal at an equimolar ratio of HPr to PRD1. Folded peaks are plotted with *dashed contour lines*. *EI* and *EII*, enzymes I and II, respectively.

Superdex 75 10/300 column (GE Healthcare) for RBD-PRD1 and GlcT H218D/H279D. The chromatography buffer consisted of 200 mM NaCl, 50 mM Tris-HCl, 5 mM $MgCl_2$ (only PRD1), and 2 mM DTT (pH 7.4).

RESULTS

HPr Phosphorylates a Histidine in the C Terminus of PRD1 in Vitro—In vitro experiments revealed that enzyme II phosphorylates PRD1 of GlcT (14). In this study, the phosphorylation of isolated PRD1 was investigated and characterized. For this purpose, PRD1 phosphorylation by enzyme I, HPr, and the cytosolic domain of the membrane-bound enzyme II was analyzed by NMR to determine optimal phosphorylation conditions. In Fig. 1, the spectral changes upon PRD1 phosphorylation, which depend on the composition of the phosphorylation enzymes, are shown in five ^{1}H,^{15}N heteronuclear single quantum correlation spectra. The spectrum of PRD1 (Fig. 1*A*) was not affected by the presence of the PTS proteins (data not shown). Thus, no protein-protein interactions between PRD1 and the phosphorylation enzymes occur in the absence of phosphoenolpyruvate. In the presence of phosphoenolpyruvate and increasing amounts of HPr, a new set of signals corresponding to phosphorylated PRD1 appeared with increasing intensity (Fig. 1, *B–E*). When HPr and PRD1 were present in equimolar amounts,

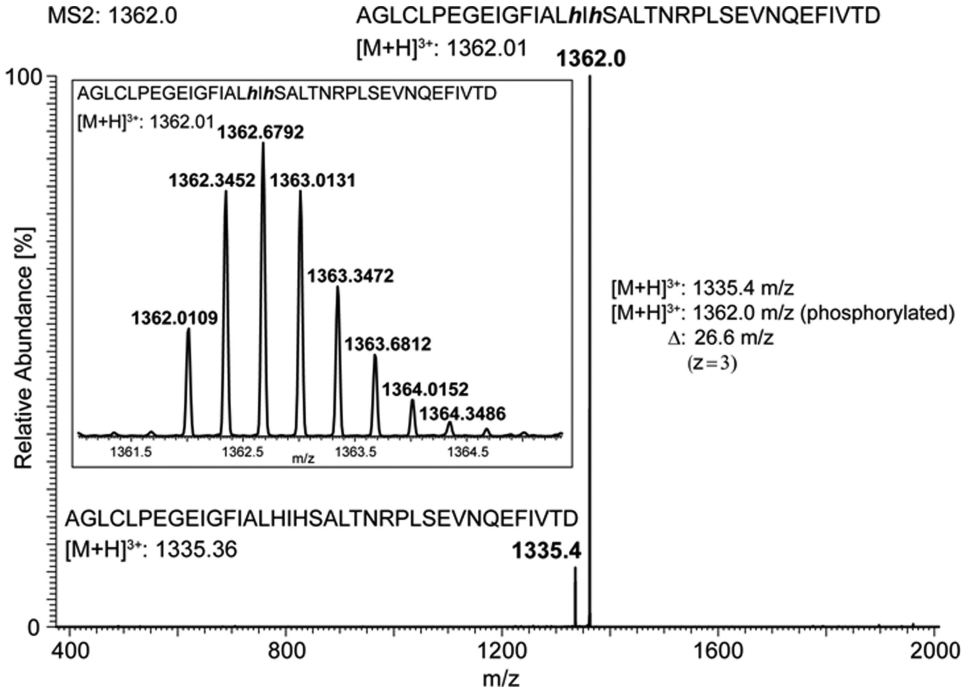

FIGURE 2. **ESI mass spectrum after tryptic digest of phosphorylated PRD1.** MS/MS analysis of PRD1 revealed His-170 and/or His-172 as being phosphorylated. The *inset* shows the MS analysis of peptide AGLCLPEGEIGFIALHIHSALTNRPLSEVNQEFIV derived from PRD1 after hydrolysis of the protein with trypsin endoproteinase (see peptide T9 in supplemental Fig. S2*B*). The mass of the triply charged peptide was determined as *m/z* 1362.0109. MS/MS analysis under higher energy collisional dissociation (*HCD*) conditions showed only a loss of 79 Da (*m/z* 26.6 as indicated to the right of the signal at *m/z* 1362.0), generating a peak at *m/z* 1335.4. The neutral loss of 79 Da is characteristic for HPO_3 and strongly suggests His-170 and/or His-172 as phosphorylation site(s). Of note, phosphorylation of serine or threonine residues always results in neutral loss of H_3PO_4 (98 Da) under collision-induced dissociation conditions. Thus, we conclude that His-170 and/or His-172 is the actual phosphorylation site of this peptide. The listed sequence of the peptide was determined by MS^3 experiments on the dephosphorylated peak at *m/z* 1335.4 (supplemental Fig. S2*C*).

nearly complete phosphorylation of PRD1 was observed (Fig. 1*E*). A control spectrum with an enzyme II-free phosphorylation mixture (supplemental Fig. S1) was identical to the spectrum of phosphorylated PRD1 (Fig. 1*E*). This result was surprising because the generally accepted model for the control of PRD-containing antiterminators suggests phosphorylation of PRD1 exclusively by enzyme II (7, 27). On the basis of our results, we conclude that HPr phosphorylates isolated PRD1 of GlcT *in vitro* and leads to the nitrogen epsilon 2 phosphorylation of a single histidine in PRD1, as shown previously (38). However, the sequence position of this specific histidine had not been determined previously.

In PRD1, two conserved histidines (His-111 and His-170) are considered to be candidates for the phosphorylation. To identify the phosphorylation site in PRD1, we performed ESI-MS^3 after tryptic digestion of the PRD1 phosphorylation mixture. A mass that was larger than expected for the non-modified peptide was measured only for the C-terminal peptide of PRD1 including His-170 (increased by 79.8 Da) (Fig. 2), suggesting that this peptide was phosphorylated at a single site. In contrast, all of the other peptides were detected with their expected mass, suggesting that the C-terminal peptide contains the unique phosphorylation site of PRD1 (supplemental Fig. S2, *A* and *B*). A neutral loss of 79.8 Da was observed upon collision-induced dissociation (Fig. 2), which clearly identified histidine phosphorylation in the C terminus of PRD1. Thus, HPr-dependent phosphorylation occurs only in the C-terminal region of recombinant PRD1, indicating His-170 as the phosphorylation site of PRD1. However, the phosphorylated peptide also contains an additional non-conserved histidine (His-172) besides the conserved His-170 (16). Therefore, we decided to determine which of the two histidines, the conserved His-170 or the non-conserved His-172, is phosphorylated.

To identify which of the two histidines is phosphorylated, we investigated a mutant of PRD1 in which His-172 was replaced with alanine (H172A). ESI-MS was performed with the PRD1 H172A phosphorylation mixture without proteolytic digestion. As shown in Fig. 3, both non-phosphorylated and phosphorylated PRD1 H172A, as well as phosphorylated HPr, were observed. A mass difference of 79.03 Da (Fig. 3, compare *species A* and *B*) clearly identified a single phosphate group (80 Da) upon *in vitro* phosphorylation of PRD1 H172A. On the basis of the observation of a single phosphorylation event, we conclude that PRD1 is phosphorylated on His-170, the second conserved histidine.

In Vivo Mutational Analysis of Histidine Residues in PRD1 of GlcT—The results presented above exclude the possibility that HPr phosphorylates His-111 of PRD1 in GlcT and favor phosphorylation of a histidine residue in the C-terminal part of PRD1. To provide *in vivo* evidence for the phosphorylation of His-170 rather than His-172, we used a series of isogenic strains in which the conserved histidine residues were individually replaced with non-phosphorylatable aspartic acid residues (Table 2). All strains contained a fusion of the *ptsG* promoter region to the promoterless *lacZ* gene encoding β-galactosidase, thus allowing an assay of GlcT activity. The resulting strains were grown in minimal medium in the presence or absence of glucose, and their β-galactosidase activities were determined.

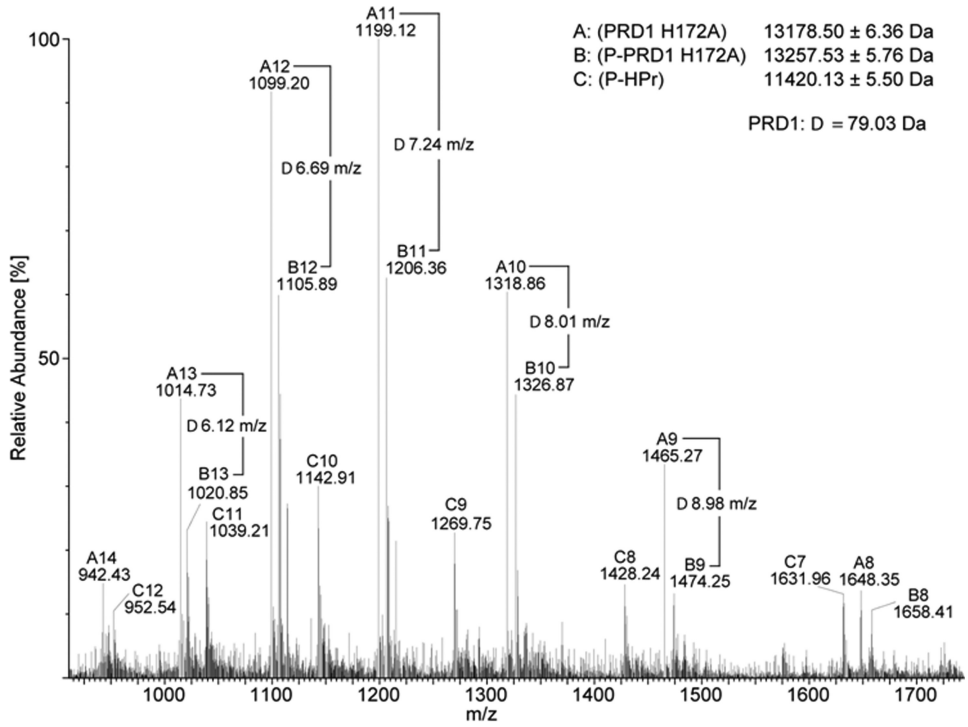

FIGURE 3. **ESI mass spectrum of phosphorylated PRD1 H172A.** A PRD1 H172A phosphorylation mixture shows non-phosphorylated PRD1 H172A (*A*, 13,178.50 ± 6.36 Da), phosphorylated PRD1 H172A (*B*, 13,257.53 ± 5.76 Da), and phosphorylated HPr (*C*, 11,420.13 ± 5.50 Da). Individual charges (*z*) of *A*, *B*, and *C* are indicated by *numbers 7-14*. A single phosphate group upon HPr-dependent PRD1 phosphorylation was identified by a mass difference of 79.03 Da.

TABLE 2
Effect of mutation of histidine residues on GlcT activity

Strain	*glcT* allele	*ptsG-lacZ* expression[a] CSE ribose	CSE glucose
		units/mg of protein	
GP771	Wild type	50 ± 30	440 ± 150
GP779	*glcT H111D*	1180 ± 320	320 ± 190
GP772	*glcT H170D*	1270 ± 120	450 ± 10
GP773	*glcT H172A*	40 ± 25	400 ± 260

[a] Representative values of *lacZ* expression are shown. All measurements were performed at least twice. The mutations are all within the boundaries of PRD1.

As shown in Table 2, the wild-type strain GP771 had a low β-galactosidase activity in the absence of glucose that was induced by ~8-fold in the presence of glucose as the inducer. This reflects the exclusive activity of GlcT in the presence of glucose and is in good agreement with previous observations (11, 14). The replacement of His-111 or His-170 with aspartic acid (GP779 and GP772, respectively) resulted in constitutive activity of GlcT. It has been shown previously that these aspartic residues are non-phosphorylatable residues in GlcT rather than mimicking histidine phosphorylation (14). Our results support the concept that these sites are required for the inactivation of GlcT by PTS-dependent phosphorylation. Again, this result is in agreement with a previous report (14). In contrast, the replacement of His-172 with the non-phosphorylatable alanine in strain GP773 had no effect on the activity of GlcT and its control in the presence or absence of glucose. Thus, this site is not involved in the control of GlcT activity. This observation is in agreement with the results in Figs. 2 and 3 showing that His-170 is the primary phosphorylation site in PRD1 of GlcT.

Phosphorylation of PRD1 Prevents Dimerization of GlcT—To investigate the quaternary structure upon HPr-dependent phosphorylation, the aggregation states of PRD1, RBD-PRD1, and GlcT H218D/H279D were investigated by size exclusion chromatography. The result is shown for isolated PRD1 in Fig. 4*A*. In the absence of phosphoenolpyruvate, dimers of PRD1 were observed. In contrast, an additional peak corresponding to monomeric PRD1 was observed upon phosphorylation (Fig. 4*A*). The identity of both aggregation states of PRD1 was confirmed by the detection of the same band from both peaks by SDS-PAGE analysis (Fig. 4*B*). In conclusion, these results clearly show that *in vitro* phosphorylation of isolated PRD1 prevents the formation of the dimer.

RBD-PRD1 was studied in a similar way to determine whether HPr is limited in its phosphorylation capability by other domains of GlcT. As observed with isolated PRD1, non-phosphorylated dimeric RBD-PRD1 was converted to a monomer upon phosphorylation (Fig. 5*A*), which was confirmed by SDS-PAGE analysis (Fig. 5, *B* and *C*). Thus, the HPr-dependent monomerization of PRD1 is not affected by the presence of the N-terminal RBD.

To gain information in the context of the full-length protein, we investigated GlcT H218D/H279D, in which PRD1 is flanked on both sides by an additional domain (N terminus, RBD; and C terminus, PRD2). To prevent HPr-dependent phosphorylation of PRD2, which has been described previously (14), the two conserved histidines in PRD2 (His-218 and His-279) were replaced with aspartic residues. Thus, phosphorylation was possible only in PRD1 of GlcT H218D/H279D. As observed for isolated PRD1 and the RBD-PRD1 construct, non-phosphorylated GlcT H218D/H279D eluted as a dimer (Fig. 6*A*). Upon phosphorylation, the monomer of GlcT H218D/H279D was observed, and the monomer/dimer ratio was even more shifted

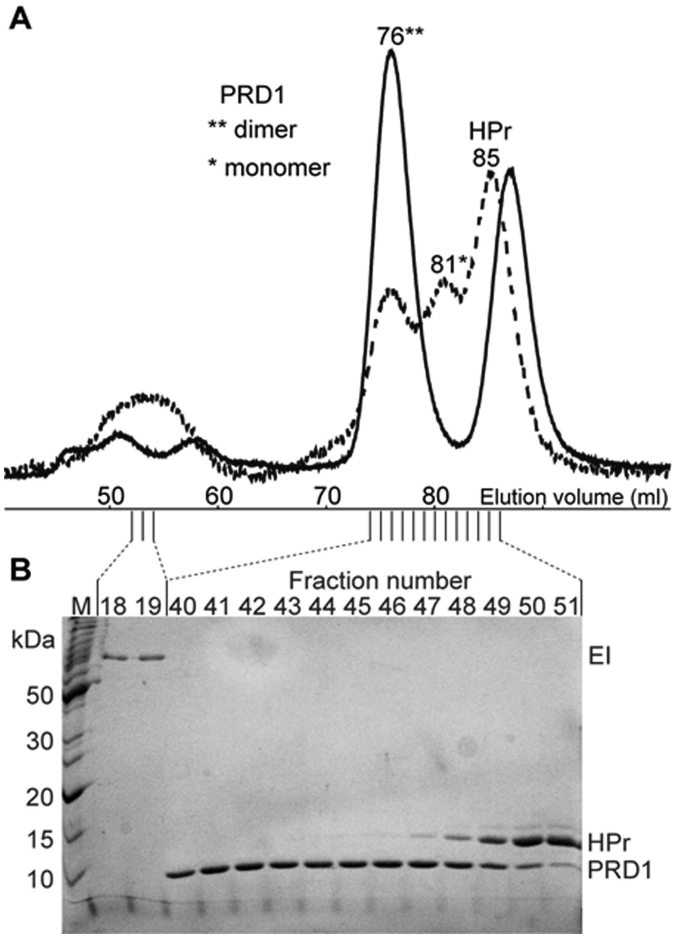

FIGURE 4. **Size exclusion chromatography elution profiles of PRD1 before and after HPr-dependent phosphorylation.** *A*, elution profiles of non-phosphorylated (*solid line*) and phosphorylated (*dashed line*) PRD1 (Superdex 75 16/60). A molar ratio of 1:1 PRD1/HPr was used for phosphorylation. Upon phosphorylation, the elution volume of the non-phosphorylated PRD1 dimer significantly changed from 76 ml to a phosphorylated monomer at 81 ml. *B*, SDS-PAGE analysis of phosphorylated PRD1. Upon phosphorylation, PRD1 was detected in both peaks (elution volumes of 76 and 81 ml), corresponding to the dimer and monomer. In the SDS-polyacrylamide gel, the band positions of HPr and PRD1 are inverted compared with their molecular masses (*lane M*). *EI*, enzyme I.

to the monomeric form with an increasing amount of HPr in the phosphorylation mixture (Fig. 6*A*, compare the *dotted* and *dashed lines*). Thus, HPr at higher concentrations was able to phosphorylate PRD1 in the context of the full-length protein, and this phosphorylation converted dimeric GlcT H218D/H279D to the monomeric form as confirmed by SDS-PAGE analysis (Fig. 6, *B* and *C*). Taken together, our data confirm that phosphorylation of PRD1 abolishes dimerization of GlcT (Fig. 7*D*).

Position of PRD1 Determines Access for HPr in Vivo—The *in vitro* phosphorylation of PRD1 by HPr was in contrast to a previous report (14). According to this report, PRD2 is the primary target of HPr, whereas PRD1 is phosphorylated by enzyme II and is only a minor substrate of HPr. To address the issue of specificity of the two conserved PRDs (PRD1 and PRD2) for two different PTS proteins, enzyme II and HPr, respectively, we performed PRD domain shuffling analysis. Briefly, we constructed and studied the activities of truncated GlcT variants that consisted of only the isolated RBD or the RBD combined with either PRD1 or PRD2 (Table 3). Moreover, we investigated the wild-type protein and one variant with an inverted arrangement of PRD1 and PRD2 (Table 3 and Fig. 7*E*). These GlcT variants were expressed constitutively from plasmids, and their effect on the regulation of *ptsG* expression was determined using a *ptsG-lacZ* fusion. This analysis was performed in strains deleted for the chromosomal copy of the *glcT* gene (GP109) (Table 3). Moreover, we used the *ptsG* mutant GP776, which lacks the glucose-specific enzyme II of the PTS, and the *ptsGHI* mutant GP777, which also lacks the general PTS proteins enzyme I and HPr. The results are summarized in Table 3.

The wild-type GlcT protein was inactive in causing antitermination in the absence of glucose, but it allowed expression of the *ptsG-lacZ* fusion if glucose was present (pGP118). In agreement with previous results (12), the wild-type protein was active even in the absence of glucose when enzyme II was absent (*i.e.* in both the *ptsG* and the *ptsGHI* mutants). Full activity was observed in the *ptsG* mutant in the presence of glucose, demonstrating that the general proteins of the PTS contribute to full GlcT activity under this condition (Fig. 7, *A–C*). The isolated RBD (pGP1063) conferred antitermination to the *ptsG* mRNA in the presence and absence of glucose in all genetic backgrounds tested. This is in agreement with previous observations (12) and confirms that the RBD itself is not subject to any control by PTS components.

The truncated GlcT protein consisting of the RBD and PRD1 (pGP1586) was inactive in the presence of the wild-type PTS proteins irrespective of the presence or absence of glucose. This inactivity might be the result of the intrinsic inactivity of the protein variant or a permanent inactivation of this protein by PTS-dependent phosphorylation events. Indeed, this truncated GlcT variant could be efficiently phosphorylated by HPr, preventing the dimerization of the protein (Fig. 5). The deletion of the *ptsG* gene did not result in activation of the truncated GlcT protein. In contrast, this protein was constitutively active in the *ptsGHI* mutant strain GP777 (Table 3). These results demonstrate unambiguously that the RBD-PRD1 construct has intrinsic activity and that the general PTS proteins cause inactivation of this truncated GlcT variant both in the presence and absence of glucose. This finding is in excellent agreement with our *in vitro* observations (Fig. 5). It demonstrates that PRD1 of GlcT is the target of HPr when present as the only PRD in GlcT.

Next, we addressed the activity of a GlcT variant composed of the RBD and PRD2 (pGP1587). This GlcT variant was active under both conditions in the absence and presence of specific and general PTS proteins. Thus, this protein did not require PTS-dependent phosphorylation for activity, and it was not inhibited by any potential phosphorylation event.

Finally, we studied the activity of a GlcT variant with an inverted arrangement of the PRDs (pGP1588). As observed before for RBD-PRD2, RBD-PRD2-PRD1 was active under all conditions tested, and the presence of PTS components had little effect, if any, on its activity. This protein may form quite stable and active dimers due to the consecutive arrangement of the RBD and PRD2, resulting in loss of control by the PTS (Fig. 7*E*). Taken together, these results indicate that HPr can indeed

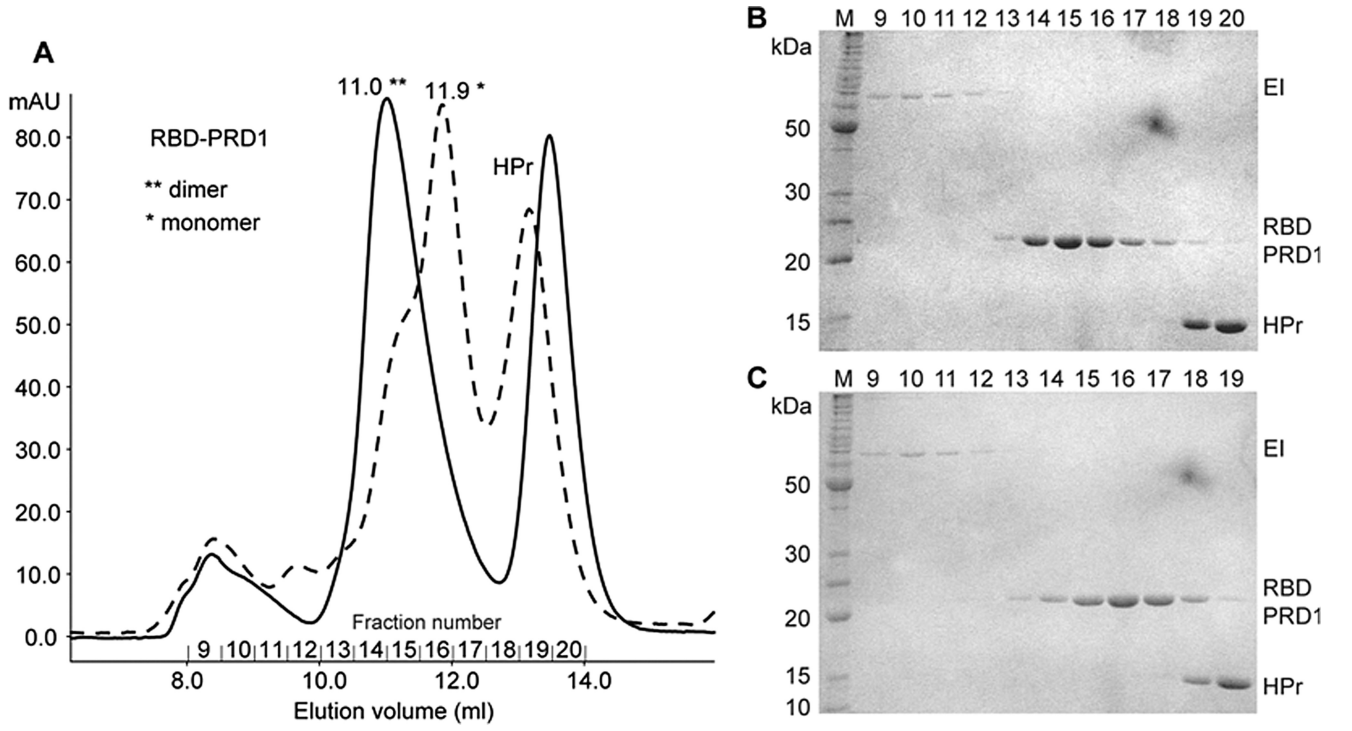

FIGURE 5. **Size exclusion chromatography elution profiles of RBD-PRD1 before and after HPr-dependent phosphorylation.** *A*, elution profiles of non-phosphorylated (*solid line*) and phosphorylated (*dashed line*) RBD-PRD1 (Superdex 75 10/300). Elution volumes and aggregation states are indicated. A molar ratio of 1:1 RBD-PRD1/HPr was used for phosphorylation. Upon phosphorylation, the elution volume of the non-phosphorylated RBD-PRD1 dimer significantly changed from 11.0 ml to a phosphorylated monomer at 11.9 ml. *mAU*, milli-absorbance units. *B* and *C*, SDS-PAGE analysis of non-phosphorylated and phosphorylated RBD-PRD1, respectively. RBD-PRD1 was identified at both elution volumes (11.0 and 11.9 ml), pointing to the dimeric and monomeric states, respectively. *M*, molecular mass markers; *EI*, enzyme I.

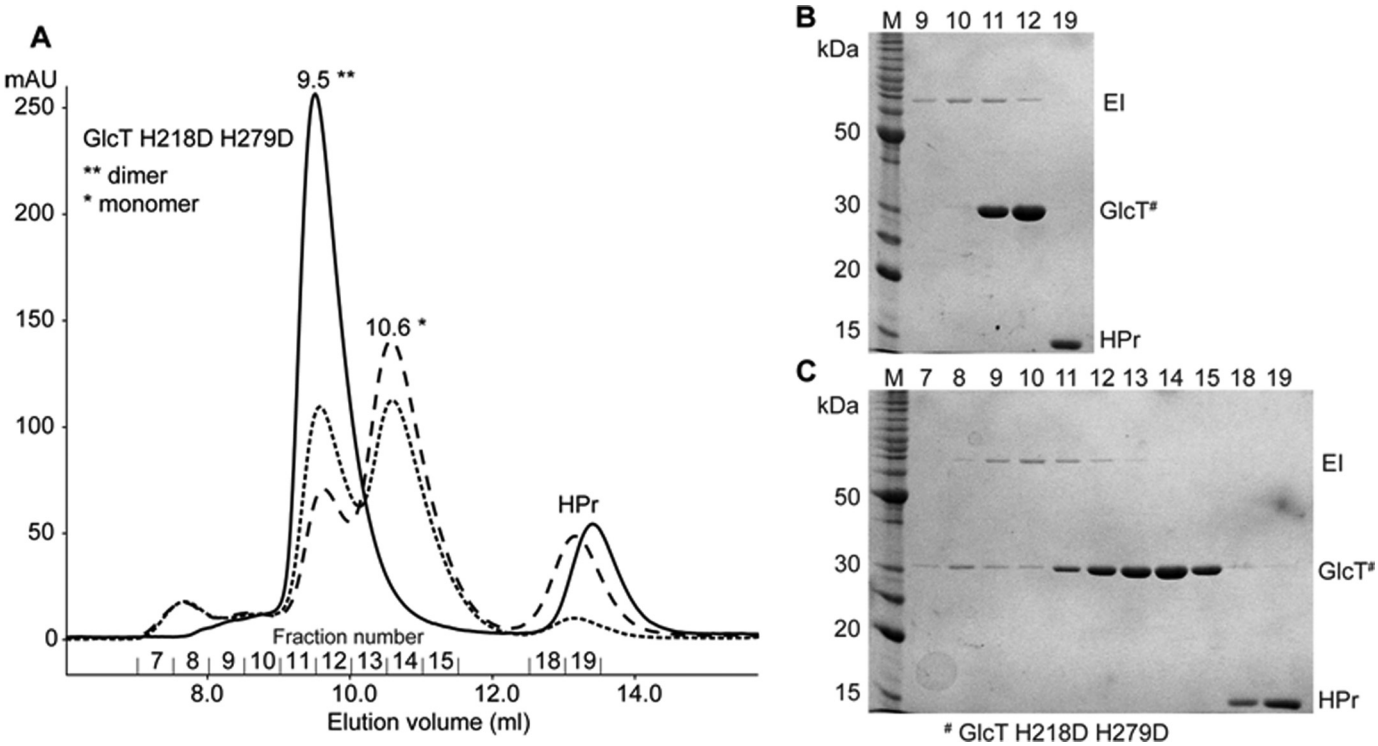

FIGURE 6. **Comparison of size exclusion chromatography elution profiles of GlcT H218D/H279D before and after HPr-dependent phosphorylation.** *A*, elution profiles of non-phosphorylated (*solid line*) and phosphorylated (*dashed* and *dotted lines*) GlcT H218D/H279D (Superdex 75 10/300). To phosphorylate GlcT H218D/H279D, 1:0.125 (*dotted line*) and 1:1 (*dashed line*) ratios of GlcT H218D/H279D to HPr were used. Upon phosphorylation, the elution volume of the non-phosphorylated GlcT H218D/H279D dimer significantly changed from 9.5 ml to a phosphorylated monomer at 10.6 ml. *mAU*, milli-absorbance units. *B* and *C*, SDS-PAGE analysis of non-phosphorylated and phosphorylated (1:1 ratio) GlcT H218D/H279D, respectively. The gels confirm the dimeric and monomeric forms of GlcT H218D/H279D before and after phosphorylation, respectively. *M*, molecular mass markers; *EI*, enzyme I.

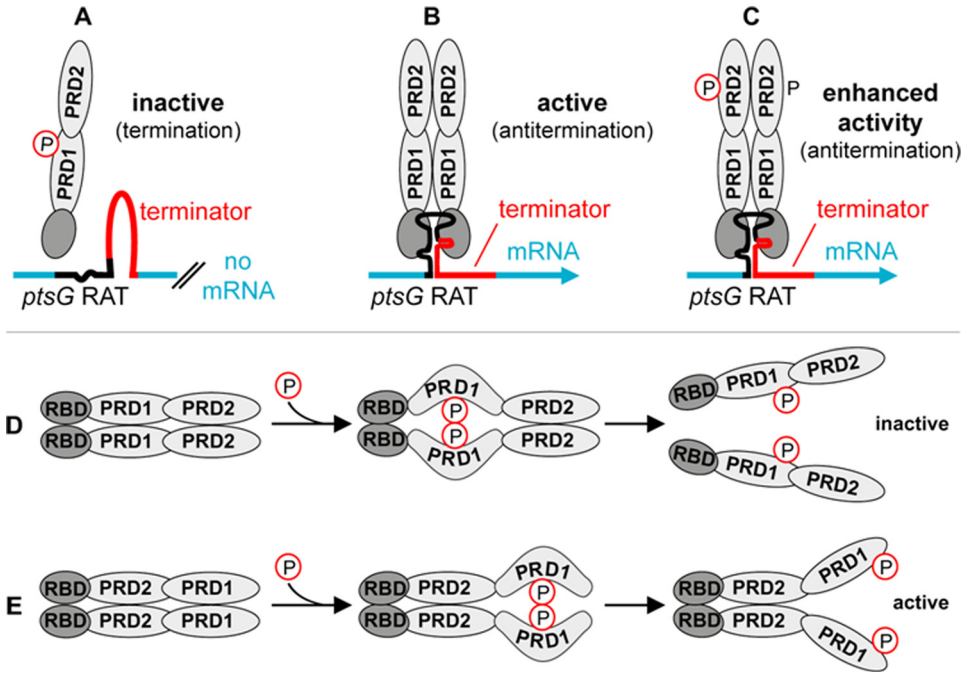

FIGURE 7. **Regulatory effects of GlcT phosphorylation and domain properties.** *A–C*, three different states of GlcT and their regulatory role in transcription termination/antitermination based on the protein-dependent RNA switch of the *ptsG* mRNA are shown. HPr- and enzyme II-dependent phosphorylation of PRD1 (*A*) prevents dimer stabilization and causes GlcT monomerization. This state results in *ptsG* expression that is equivalent to ~20–50 units of β-galactosidase (Table 3). Non-phosphorylated GlcT (*B*) intrinsically binds the *ptsG* RNA antiterminator (*RAT*) sequence to prevent transcription termination. This antitermination scenario is enhanced by HPr-dependent phosphorylation of PRD2 (*C*). These forms of GlcT allow *ptsG* expression levels that correspond to 300–700 or >800 units of β-galactosidase, respectively (see Table 3). *D* and *E*, the impact of phosphorylation of PRD1 is shown for GlcT and a GlcT variant with shuffled PRDs, respectively. The domain organization of the RBD, PRD1, and PRD2 ensures that upon PRD1 phosphorylation, the GlcT dimers dissociate to the inactive monomers. In contrast, the intrinsic ability of PRD2 to form a stable dimer enhances the stability of the shuffled GlcT variant, resulting in constitutive antitermination, irrespective of the PRD1 phosphorylation state.

TABLE 3
Effect of domain arrangement and PTS proteins on GlcT activity

		ptsG-lacZ expression[a,b]					
		GP109 (Δ*glcT8*) (enzyme I, HPr, and enzyme II)[c]		GP776 (Δ*glcT* Δ*ptsG*) (enzyme I and HPr)[c]		GP777 (Δ*glcT* Δ*ptsGHI*) (none)[c]	
Plasmid	GlcT variant	−Glc	+Glc	−Glc	+Glc	−Glc	+Glc
		units/mg of protein					
pGP118	Wild-type RBD-PRD1-PRD2	30 ± 15	502 ± 200	376 ± 60	1049 ± 60	437 ± 20	494 ± 25
pGP1063	RBD	1144 ± 270	1077 ± 320	1100 ± 10	966 ± 230	1020 ± 25	1025 ± 50
pGP1586	RBD-PRD1	23 ± 5	35 ± 10	23 ± 4	29 ± 2	547 ± 210	594 ± 25
pGP1587	RBD-PRD2	1096 ± 197	1025 ± 120	1360 ± 90	1217 ± 5	1261 ± 130	1769 ± 120
pGP1588	RBD-PRD2-PRD1	596 ± 2	367 ± 100	707 ± 110	598 ± 60	824 ± 50	803 ± 20

[a] Representative values of *lacZ* expression are shown. All measurements were performed at least twice.
[b] β-Galactosidase activities in the range of 20–50 units correspond to the inactive GlcT protein (Fig. 7*A*). Values from 300 to 700 units are characteristic for the active GlcT protein (Fig. 7*B*), and values >800 indicate enhanced activity of GlcT (Fig. 7*C*).
[c] Chromosomally encoded PTS proteins.

target the PRD1 of GlcT when this PRD is positioned at the C terminus.

DISCUSSION

Gene regulation often involves responses to multiple signals. Classically, the information is sensed and transduced by a specialized regulator. This is the case in the paradigm of bacterial gene regulation, the *E. coli* lactose operon. However, some regulatory proteins have the ability to combine distinct inputs and to integrate this information to a coordinated output as observed in the PRD-containing regulator proteins in bacteria. These regulators control the expression of sugar utilization genes, and the activity of each of the regulators is modulated by the availability of both the specific substrate and the preferred carbon source, glucose (7, 39). This dual information input is achieved by the independent control of the two conserved PRDs by antagonistically acting PTS-dependent phosphorylation events. In all PRD-containing antitermination proteins studied so far, PRD1 is thought to be phosphorylated by the cognate sugar-specific enzyme II, whereas PRD2 is the subject of HPr-dependent phosphorylation. This assignment of phosphorylating PTS proteins to their phosphorylation targets in an antiterminator was demonstrated for the *B. subtilis* GlcT protein *in vivo* and *in vitro* (14). However, this raises the immediate question of how signaling specificity for the PRDs is achieved.

A large body of genetic evidence supports the assignment of HPr and enzyme II to their cognate PRDs (12, 14, 22, 40, 41). However, some previous studies suggest that HPr may phos-

phorylate even PRD1 of LicT and GlcT (14, 41, 42). In GlcT, this HPr-dependent phosphorylation of PRD1 was very inefficient compared with enzyme II-dependent phosphorylation. The results presented in this study confirm that HPr is capable of phosphorylating PRD1 of GlcT. In general, efficient phosphorylation among the PTS proteins requires only catalytic amounts of the phosphorylating phosphotransferases; in contrast, at least equimolar amounts of HPr are needed to observe efficient phosphorylation of PRD1 (Fig. 1). This lower affinity between HPr and PRD1 is in good agreement with the preference of HPr for PRD2 (14). Indeed, an ~10-fold excess of HPr molecules is necessary to phosphorylate PRD1 as efficiently as PRD2 (supplemental Fig. S3). Thus, a catalytic mechanism of PRD phosphorylation by HPr is supported by the combined results obtained *in vitro* by gel electrophoresis (using radioactively labeled phosphoenolpyruvate) (14), NMR analysis (Fig. 1), ESI-MS (Fig. 2), and gel filtration (supplemental Fig. S3).

The observation that HPr can phosphorylate PRD1, even though with reduced efficiency, calls for specificity determinants that control the interaction of the PRDs with HPr and enzyme II. A possible answer to this question can be derived from our studies with GlcT variants with altered PRD arrangements (Table 3 and Fig. 7, *D* and *E*). The wild-type GlcT protein is inactive in the absence of glucose due to enzyme II-dependent phosphorylation of PRD1 (Fig. 7*A*) (14). Accordingly, inactivation of the *ptsG* gene, encoding the glucose-specific enzyme II, results in the constitutive activity of GlcT. This activity is not further increased if all PTS proteins are absent (Table 3). Thus, HPr is unable to replace enzyme II in the negative control of GlcT by phosphorylation of PRD1 *in vivo*. Completely different pictures emerged when the RBD is fused to either PRD1 or PRD2. The protein consisting of RBD-PRD1 is inactive as long as the general PTS components are present in the cell; in contrast, this GlcT variant allows antitermination of the *ptsG* mRNA in the absence of HPr (Table 3). This suggests that this domain configuration, namely the absence of PRD2, putting PRD1 at the C terminus of GlcT, allows HPr to control the regulatory output of this truncated GlcT variant by phosphorylation of PRD1. One may ask whether the experimental setup using truncated GlcT proteins is biologically relevant because such proteins never occur in nature. However, analysis of the particular specific domains is possible only in such a setup, as this allows the study of the distinct interactions of the two PRDs with the two different PTS proteins, HPr and enzyme II. PRD1 intrinsically forms dimers, and phosphorylation results in monomerization (Fig. 4). This is in perfect agreement with the fact that the RBD-PRD1 construct is only active as an antiterminator when no HPr-dependent phosphorylation is possible. In contrast, the GlcT construct consisting of the RBD and PRD2 is active as a antiterminator under all conditions, even in the absence of any PTS-dependent phosphorylation in the *ptsGHI* mutant strain. In this respect, this GlcT variant is indistinguishable from the isolated RBD. However, it is well established that PRD2 of GlcT can be phosphorylated by HPr but that this phosphorylation has only a slight enhancing effect on GlcT activity (14). Thus, HPr-dependent phosphorylation of the RBD-PRD2 variant is possible but has little impact, if any, on the final activity of the protein. Therefore, we conclude that our findings are best explained by the hypothesis that, *in vivo*, HPr can effectively access only PRDs at the very C terminus of the antitermination proteins.

Another interesting implication of our results concerns the intrinsic properties of the two PRDs. PRD1 normally forms dimers and can be forced to a monomeric conformation only by phosphorylation (Fig. 7*D*). In contrast, non-phosphorylated PRD2 of GlcT forms monomers as well as dimers, and the tendency to dimerize is even increased upon phosphorylation (Fig. 7, *B* and *C*). These properties of the two domains are still observed when the single PRDs are fused to the RBD. Moreover, the PRDs confer their specific monomerization/dimerization properties to the GlcT protein irrespective of the domain arrangement (Table 3). Even the constitutive activity of the GlcT variant with an inverted PRD arrangement can be explained with the dimerization behavior of the PRDs (Fig. 7*E*).

The domain arrangement of GlcT and the other antitermination proteins of the BglG/SacY family provides an easy explanation for the integration of general and specific signals in one regulator protein. Although HPr can phosphorylate PRD2 of all antitermination proteins, the sugar-specific enzyme II phosphorylates and thereby inactivates only its specific cognate PRD1 target. Compared with PRD2, PRD1 is ~10-fold less efficiently phosphorylated by HPr. Thus, *in vivo*, HPr phosphorylates preferably different C-terminal PRD2 domains. This versatility of interaction between HPr and the PRD2 domains of all antitermination proteins is in good agreement with the flexibility of HPr to interact with a wide range of different proteins, including enzyme I and several classes of enzymes II of the PTS; the HPr kinase; the CcpA, RbsR, and YesS transcription factors; the PRD-type regulators; and metabolic enzymes such as glyceraldehyde-3-phosphate dehydrogenase and glycerol kinase (7, 43–48). In contrast, the different enzymes II seem to recognize specific features based on the distinct amino acid sequences and the derived structures of their cognate PRD1 (16). This reflects the substrate specificity of these proteins and their limited ability to interact with non-cognate proteins.

In conclusion, the conserved organization of the regulatory PRDs in GlcT and most likely also in the other antitermination proteins is essential to provide the activity control of these proteins and serves as a crucial specificity determinant. This explains the conservation of the domain arrangement among the various antitermination proteins: even if PRD2 can dimerize in the absence of HPr-mediated phosphorylation as in GlcT, the general domain organization of these regulators seems to be under evolutionary pressure.

To further investigate the selectivity of the interactions between HPr and enzyme II with PRD2 and PRD1, respectively, it will be interesting to isolate PRD variants that affect this interaction specificity. This approach has already proven valuable for the RBD-RNA interactions (30) and will certainly provide novel insights into the constraints that keep the complex signaling chains to the antitermination proteins straight.

Acknowledgments—We are grateful to Christina Herzberg for expert technical assistance and Gerhard Wolf for recording and processing the mass spectra of PRD1 H172A.

REFERENCES

1. Matthews, K. S. (1996) The whole lactose repressor. *Science* **271,** 1245–1246
2. Deutscher, J., Küster, E., Bergstedt, U., Charrier, V., and Hillen, W. (1995) Protein kinase-dependent HPr/CcpA interaction links glycolytic activity to carbon catabolite repression in Gram-positive bacteria. *Mol. Microbiol.* **15,** 1049–1053
3. Elsholz, A. K., Michalik, S., Zühlke, D., Hecker, M., and Gerth, U. (2010) CtsR, the Gram-positive master regulator of protein quality control, feels the heat. *EMBO J.* **29,** 3621–3629
4. Gao, R., and Stock, A. M. (2010) Molecular strategies for phosphorylation-mediated regulation of response regulator activity. *Curr. Opin. Microbiol.* **13,** 160–167
5. Stülke, J., Arnaud, M., Rapoport, G., and Martin-Verstraete, I. (1998) PRD–a protein domain involved in PTS-dependent induction and carbon catabolite repression of catabolic operons in bacteria. *Mol. Microbiol.* **28,** 865–874
6. Declerck, N., Dutartre, H., Receveur, V., Dubois, V., Royer, C., Aymerich, S., and van Tilbeurgh, H. (2001) Dimer stabilization upon activation of the transcriptional antiterminator LicT. *J. Mol. Biol.* **314,** 671–681
7. Deutscher, J., Francke, C., and Postma, P. W. (2006) How phosphotransferase system-related protein phosphorylation regulates carbohydrate metabolism in bacteria. *Microbiol. Mol. Biol. Rev.* **70,** 939–1031
8. Amster-Choder, O., and Wright, A. (1990) Regulation of activity of a transcriptional antiterminator in *E. coli* by phosphorylation *in vivo*. *Science* **249,** 540–542
9. Schnetz, K., and Rak, B. (1990) β-Glucoside permease represses the *bgl* operon of *Escherichia coli* by phosphorylation of the antiterminator protein and also interacts with glucose-specific enzyme III, the key element in catabolite control. *Proc. Natl. Acad. Sci. U.S.A.* **87,** 5074–5078
10. Débarbouillé, M., Martin-Verstraete, I., Klier, A., and Rapoport, G. (1991) The transcriptional regulator LevR of *Bacillus subtilis* has domains homologous to both σ54- and phosphotransferase system-dependent regulators. *Proc. Natl. Acad. Sci. U.S.A.* **88,** 2212–2216
11. Stülke, J., Martin-Verstraete, I., Zagorec, M., Rose, M., Klier, A., and Rapoport, G. (1997) Induction of the *Bacillus subtilis ptsGHI* operon by glucose is controlled by a novel antiterminator, GlcT. *Mol. Microbiol.* **25,** 65–78
12. Bachem, S., and Stülke, J. (1998) Regulation of the *Bacillus subtilis* GlcT antiterminator protein by components of the phosphotransferase system. *J. Bacteriol.* **180,** 5319–5326
13. Langbein, I., Bachem, S., and Stülke, J. (1999) Specific interaction of the RNA-binding domain of the *Bacillus subtilis* transcriptional antiterminator GlcT with its RNA target, RAT. *J. Mol. Biol.* **293,** 795–805
14. Schmalisch, M. H., Bachem, S., and Stülke, J. (2003) Control of the *Bacillus subtilis* antiterminator protein GlcT by phosphorylation. Elucidation of the phosphorylation chain leading to inactivation of GlcT. *J. Biol. Chem.* **278,** 51108–51115
15. Manival, X., Yang, Y., Strub, M. P., Kochoyan, M., Steinmetz, M., and Aymerich, S. (1997) From genetic to structural characterization of a new class of RNA-binding domain within the SacY/BglG family of antiterminator proteins. *EMBO J.* **16,** 5019–5029
16. Greenberg, D. B., Stülke, J., and Saier, M. H. (2002) Domain analysis of transcriptional regulators bearing PTS regulatory domains. *Res. Microbiol.* **153,** 519–526
17. Commichau, F. M., and Stülke, J. (2008) Trigger enzymes: bifunctional proteins active in metabolism and in controlling gene expression. *Mol. Microbiol.* **67,** 692–702
18. Galinier, A., Kravanja, M., Engelmann, R., Hengstenberg, W., Kilhoffer, M. C., Deutscher, J., and Haiech, J. (1998) New protein kinase and protein phosphatase families mediate signal transduction in bacterial catabolite repression. *Proc. Natl. Acad. Sci. U.S.A.* **95,** 1823–1828
19. Reizer, J., Hoischen, C., Titgemeyer, F., Rivolta, C., Rabus, R., Stülke, J., Karamata, D., Saier, M. H., Jr., and Hillen, W. (1998) A novel protein kinase that controls carbon catabolite repression in bacteria. *Mol. Microbiol.* **27,** 1157–1169
20. Singh, K. D., Schmalisch, M. H., Stülke, J., and Görke, B. (2008) Carbon catabolite repression in *Bacillus subtilis*: quantitative analysis of repression exerted by different carbon sources. *J. Bacteriol.* **190,** 7275–7284
21. Görke, B., and Rak, B. (1999) Catabolite control of *Escherichia coli* regulatory protein BglG activity by antagonistically acting phosphorylations. *EMBO J.* **18,** 3370–3379
22. Görke, B. (2003) Regulation of the *Escherichia coli* antiterminator protein BglG by phosphorylation at multiple sites and evidence for transfer of phosphoryl groups between monomers. *J. Biol. Chem.* **278,** 46219–46229
23. Raveh, H., Lopian, L., Nussbaum-Shochat, A., Wright, A., and Amster-Choder, O. (2009) Modulation of transcription antitermination in the *bgl* operon of *Escherichia coli* by the PTS. *Proc. Natl. Acad. Sci. U.S.A.* **106,** 13523–13528
24. Arnaud, M., Vary, P., Zagorec, M., Klier, A., Débarbouillé, M., Postma, P., and Rapoport, G. (1992) Regulation of the *sacPA* operon of *Bacillus subtilis*: identification of phosphotransferase system components involved in SacT activity. *J. Bacteriol.* **174,** 3161–3170
25. Déméné, H., Ducat, T., De Guillen, K., Birck, C., Aymerich, S., Kochoyan, M., and Declerck, N. (2008) Structural mechanism of signal transduction between the RNA-binding domain and the phosphotransferase system regulation domain of the LicT antiterminator. *J. Biol. Chem.* **283,** 30838–30849
26. Graille, M., Zhou, C. Z., Receveur-Bréchot, V., Collinet, B., Declerck, N., and van Tilbeurgh, H. (2005) Activation of the LicT transcriptional antiterminator involves a domain swing/lock mechanism provoking massive structural changes. *J. Biol. Chem.* **280,** 14780–14789
27. van Tilbeurgh, H., and Declerck, N. (2001) Structural insights into the regulation of bacterial signaling proteins containing PRDs. *Curr. Opin. Struct. Biol.* **11,** 685–693
28. Schilling, O., Herzberg, C., Hertrich, T., Vörsmann, H., Jessen, D., Hübner, S., Titgemeyer, F., and Stülke, J. (2006) Keeping signals straight in transcription regulation: specificity determinants for the interaction of a family of conserved bacterial RNA-protein couples. *Nucleic Acids Res.* **34,** 6102–6115
29. Schilling, O., Langbein, I., Müller, M., Schmalisch, M. H., and Stülke, J. (2004) A protein-dependent riboswitch controlling *ptsGHI* operon expression in *Bacillus subtilis*: RNA structure rather than sequence provides interaction specificity. *Nucleic Acids Res.* **32,** 2853–2864
30. Hübner, S., Declerck, N., Diethmaier, C., Le Coq, D., Aymerich, S., and Stülke, J. (2011) Prevention of cross-talk in conserved regulatory systems: identification of specificity determinants in RNA-binding antitermination proteins of the BglG family. *Nucleic Acids Res.* **39,** 4360–4372
31. Commichau, F. M., Herzberg, C., Tripal, P., Valerius, O., and Stülke, J. (2007) A regulatory protein-protein interaction governs glutamate biosynthesis in *Bacillus subtilis*: the glutamate dehydrogenase RocG moonlights in controlling the transcription factor GltC. *Mol. Microbiol.* **65,** 642–654
32. Sambrook, J., Fritsch, E. F., and Maniatis, T. (1989) *Molecular Cloning: A Laboratory Manual*, 2nd Ed., Cold Spring Harbor Laboratory, Cold Spring Harbor, NY
33. Kunst, F., and Rapoport, G. (1995) Salt stress is an environmental signal affecting degradative enzyme synthesis in *Bacillus subtilis*. *J. Bacteriol.* **177,** 2403–2407
34. Martin-Verstraete, I., Débarbouillé, M., Klier, A., and Rapoport, G. (1994) Interactions of wild-type and truncated LevR of *Bacillus subtilis* with the upstream activating sequence of the levanase operon. *J. Mol. Biol.* **241,** 178–192
35. Bi, W., and Stambrook, P. J. (1998) Site-directed mutagenesis by combined chain reaction. *Anal. Biochem.* **256,** 137–140
36. Guérout-Fleury, A. M., Shazand, K., Frandsen, N., and Stragier, P. (1995) Antibiotic-resistance cassettes for *Bacillus subtilis*. *Gene* **167,** 335–336
37. Wach, A. (1996) PCR synthesis of marker cassettes with long flanking homology regions for gene disruptions in *S. cerevisiae*. *Yeast* **12,** 259–265
38. Himmel, S., Wolff, S., Becker, S., Lee, D., and Griesinger, C. (2010) Detection and identification of protein phosphorylation sites in histidines through HNP correlation patterns. *Angew. Chem. Int. Ed. Engl.* **49,** 8971–8974
39. Görke, B., and Stülke, J. (2008) Carbon catabolite repression in bacteria: many ways to make the most out of nutrients. *Nat. Rev. Microbiol.* **6,** 613–624

40. Lindner, C., Hecker, M., Le Coq, D., and Deutscher, J. (2002) *Bacillus subtilis* mutant LicT antiterminators exhibiting enzyme I- and HPr-independent antitermination affect catabolite repression of the *bglPH* operon. *J. Bacteriol.* **184,** 4819–4828
41. Tortosa, P., Declerck, N., Dutartre, H., Lindner, C., Deutscher, J., and Le Coq, D. (2001) Sites of positive and negative regulation in the *Bacillus subtilis* antiterminators LicT and SacY. *Mol. Microbiol.* **41,** 1381–1393
42. Lindner, C., Galinier, A., Hecker, M., and Deutscher, J. (1999) Regulation of the activity of the *Bacillus subtilis* antiterminator LicT by multiple PEP-dependent, enzyme I- and HPr-catalyzed phosphorylation. *Mol. Microbiol.* **31,** 995–1006
43. Poncet, S., Soret, M., Mervelet, P., Deutscher, J., and Noirot, P. (2009) Transcriptional activator YesS is stimulated by histidine-phosphorylated HPr of the *Bacillus subtilis* phosphotransferase system. *J. Biol. Chem.* **284,** 28188–28197
44. Pompeo, F., Luciano, J., and Galinier, A. (2007) Interaction of GapA with HPr and its homolog, Crh: novel levels of regulation of a key step of glycolysis in *Bacillus subtilis*? *J. Bacteriol.* **189,** 1154–1157
45. Müller, W., Horstmann, N., Hillen, W., and Sticht, H. (2006) The transcriptional regulator RbsR represents a novel interaction partner of the phosphoprotein HPr-Ser46-P in *Bacillus subtilis*. *FEBS J.* **273,** 1251–1261
46. Schumacher, M. A., Allen, G. S., Diel, M., Seidel, G., Hillen, W., and Brennan, R. G. (2004) Structural basis for allosteric control of the transcription regulator CcpA by the phosphoprotein HPr-Ser46-P. *Cell* **118,** 731–741
47. Fieulaine, S., Morera S., Poncet, S., Mijakovic, I., Galinier, A., Janin, J., Deutscher, J., and Nessler, S. (2002) X-ray structure of a bifunctional protein kinase in complex with its protein substrate HPr. *Proc. Natl. Acad. Sci. U.S.A.* **99,** 13437–13441
48. Darbon, E., Servant, P., Poncet, S., and Deutscher, J. (2002) Antitermination by GlpP, catabolite repression via CcpA, and inducer exclusion triggered by P~GlpK dephosphorylation control *Bacillus subtilis glpFK* expression. *Mol. Microbiol.* **43,** 1039–1052